INTERFACE PHENOMENA AND DIELECTRIC PROPERTIES OF BIOLOGICAL TISSUE

Ørjan G. Martinsen
University of Oslo, Blindern Oslo, Norway

Sverre Grimnes
University of Oslo, Blindern Oslo, Norway
Rikshospitalet, Oslo, Norway

Herman P. Schwan
University of Pennsylvania, Philadelphia, Pennsylvania, U.S.A.

INTRODUCTION

The dielectric properties of biological cells and tissues are very remarkable. They typically display extremely high dielectric constants at low frequencies, falling off in more or less distinct steps as the excitation frequency is increased. Their frequency dependence permits identification and investigation of a number of completely different underlying mechanisms, and hence, dielectric studies of biomaterials have long been important in electrophysiology and biophysics. As an example, Höber (1, 2) deduced from dielectric studies that erythrocytes are composed of a poorly conducting envelope enclosing a conducting electrolyte, and in 1925, Fricke (3) derived a value of 3.3 nm for the thickness of this envelope. Hence their bioimpedance research provided early indication of the ultrathin cell membrane.

As we shall see later, interfaces play a significant role in the frequency dependence of complex materials, particularly at audio and subaudio frequencies.

RELAXATION AND DISPERSION

Electric *polarization* may be defined as the electric field-induced disturbance of the charge distribution in a region (4). This polarization does not occur instantaneously, and the associated time constant is called the *relaxation time* τ. The relaxation time for a system can be measured by applying a step function as excitation and then monitoring the relaxation process toward a new equilibrium in the time domain. The relaxation of electrons and small dipolar molecules is a relatively fast process, with relaxation times in the pico- and nanosecond range, while interfacial polarization may give relaxation times of the order of seconds.

Dielectric *dispersion* is the corresponding frequency dependence of permittivity. In Fig. 1, the real part of the relative permittivity drops off in distinct steps as the frequency increases. A dispersion will then be the transition from one level to another, where the median value between these two levels will occur at the *characteristic frequency* $f_c = 1/2\pi\tau$. In biological tissue, these dispersions may be more or less discernible.

At first glance the electrical properties of tissues and cell suspensions could be expressed by logarithmic frequency dependence over the whole frequency range from a few Hertz to many gigaHertz. This sort of behavior is not unexpected for fractal systems, and tissues would certainly qualify on that account. Schwan (5) measured tissue and cell suspension electrical properties over a much broader frequency range, which had become available for such purposes after World War II. He observed that the properties are characterized by three major dispersions, which he termed α-β-γ and that different mechanisms account for low frequency (α), radio frequency (β), and microwave frequency (γ) data. Finally, additional smaller magnitude fine structure effects lead to further differentiation since low-frequency, radio frequency, and microwave effects in turn exhibit multiple relaxational behavior.

The radio frequency (β) dispersion was first investigated and recognized as a Maxwell-Wagner relaxation caused by cell membranes (6). A large-magnitude, low-frequency dispersion was observed by Schwan with muscle tissue (7) and is related in part at least to the tubular system (8). Colloidal particle suspensions also display this phenomenon (9, 10). It is caused by the counterion

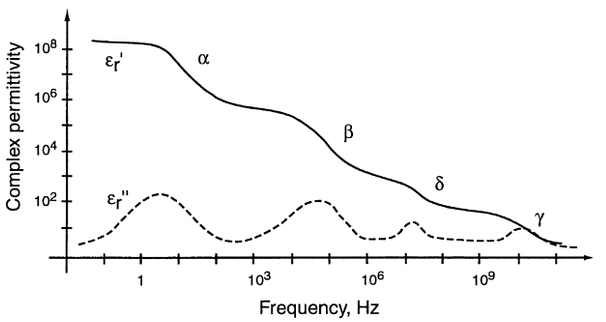

Fig. 1 Idealised dispersion regions for tissue. Dc conductance contribution has been subtracted from the ε_r'' values shown.

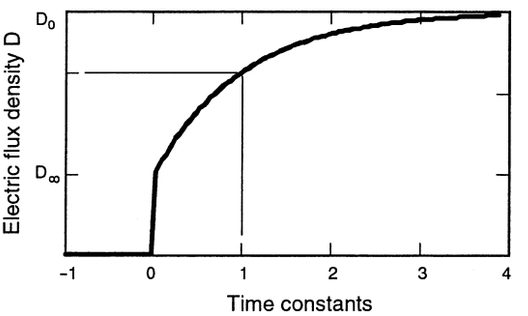

Fig. 2 Electric flux density in the capacitor dielectric with an applied voltage step.

atmosphere surrounding the charged particle surface. A first theory of this counterion relaxation was published by Schwarz (11).

Rajewsky and Schwan (12) noted a third dispersion at microwave frequencies. It is caused by abundant tissue water. Several effects of smaller magnitude were later added by Schwan (13). Membrane relaxation is anticipated from the Hodgkin-Huxley membrane model (14, 15) and adds to the α-effects caused by the sarcoplasmic reticulum, gap junctions, and counterion relaxation. A number of β-effects of small magnitude occur at the tail of the β-dispersion. These effects are caused by proteins, protein-bound water (δ-dispersion), and cell organelles such as mitochondria (16). A second Maxwell-Wagner dispersion is characteristic of suspended particles surrounded by a shell and usually of small magnitude (17). It occurs at frequencies well above those of the main β-dispersion.

The maximum dispersion magnitudes for tissue given by Schwan (18), shown in Table 1, agree well with the useful control equation, which gives the relationship between $\Delta\varepsilon$, τ, and $\Delta\sigma$:

$$\Delta\varepsilon' = \tau\Delta\sigma' = \frac{\Delta\sigma'}{\omega_c} \tag{1}$$

where $f_c = \omega_c/2\pi$. The conductivity in this equation does not account for dc conductivity, only for dielectric loss. The possible mechanisms behind these dispersions will be discussed for different systems and tissues later in this article.

Table 1 Maximum dispersion magnitudes

	α	β	γ
$\Delta\varepsilon_r$	5×10^6	10^5	75
$\Delta\sigma$	10^{-2}	1	80

In the simplest case of a medium with a single relaxation mechanism (Debye type (19)), the system will relax toward a new equilibrium as a first-order process, characterized by a relaxation time τ:

$$D(t) = D_\infty + \frac{D_0 - D_\infty}{1 - e^{-t/\tau}} \tag{2}$$

Eq. 2 and Fig. 2 shows how the electric flux density in the material increases from one value (D_∞) to another (D_0) after a step in the applied voltage at $t = 0$. The subscripts refer to frequency, so that D_∞ is the flux density at $t = 0+$, representing the apparently instantaneous polarization of the medium when the voltage step is applied (high frequency), and D_0 is the steady state (or static) value obtained after a time $t >> \tau$ (low frequency).

By Laplace transforming Eq. 2 it is possible to obtain the response in the frequency domain. With the real part of the permittivity $\varepsilon' = D/E$ and $C = \varepsilon' A/d$ (E is electric field strength, C is capacitance, A is the cross section of the medium, and d is its thickness), it is possible to show that

$$\bar{\varepsilon}(\omega) = \varepsilon'_\infty + \frac{\Delta\varepsilon'}{1 + j\omega\tau} \quad \text{where} \quad \Delta\varepsilon' = \varepsilon'_S - \varepsilon'_\infty \tag{3}$$

$$\overline{C}(\omega) = C_\infty + \frac{\Delta C}{1 + j\omega\tau} \quad \text{where} \quad \Delta C = C_0 - C_\infty \tag{4}$$

The subscript s for ''static'' is used, since ε_0 is reserved for the permittivity of vacuum. Hence, as the frequency increases, the permittivity (and capacitance) drops from one stable value ε_s to another ε_∞ over roughly one decade in frequency. The permittivity is halfway between the two limiting values at the characteristic frequency f_c. A drop in permittivity is associated with an increase in conductivity according to the general Kramers-Kronig relation:

$$\sigma_\infty - \sigma_s = \frac{\varepsilon_s - \varepsilon_\infty}{\tau} \tag{5}$$

In most real systems, and particularly in complex systems like biomaterials, the transition from one permittivity value to another will occur over a frequency band that is broader than for this idealized system. This is normally interpreted as being due to a distribution of relaxation times, e.g., because of the distribution of cell sizes in the studied biomaterial. Studying the material over a broad frequency range may also reveal more than one dispersion if several relaxation mechanisms are involved and their time constants are sufficiently different.

Maxwell-Wagner Effects

The Maxwell-Wagner effect is an interfacial relaxation process occurring in all systems where the electric current must pass an interface between two different dielectrics. This is often illustrated by means of a plate capacitor with two different homogenous materials inserted as slabs in series between the capacitor plates. Fig. 3 shows the capacitor with a simple dielectric model.

If the resultant parallel capacitance C_p is calculated, we get

$$C_p = (C_1R_1^2 + C_2R_2^2)/(R_1 + R_2)^2 \quad f \to 0$$
$$C_p = C_1C_2/(C_1 + C_2) \quad f \to \infty \tag{6}$$

The capacitance values converge both at low and high frequencies, and the capacitance at low frequency is higher than that at high frequency. Thus with the parallel model of two slabs in series, we have a classical Debye dispersion even without any dipole relaxation in the dielectric. The dispersion is due to a conductance in parallel with a capacitance for each dielectric, so that the interface can be charged by the conductivity. In an interface without free charges, the dielectric displacement $\overline{D}$ is continuous across the interface according to Poisson's equation.

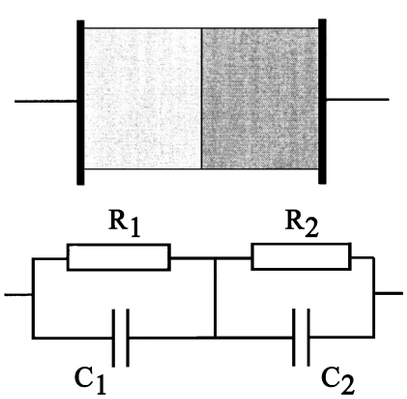

Fig. 3 Equivalent circuit for the Maxwell-Wagner effect in a simple dielectric model.

Since $\overline{D} = \varepsilon\overline{E}$, this indicates that the electric field strength will be smaller on the high-permittivity side. The ratio of current densities on sides 1 and 2 will then be equal to 1:

$$\frac{J_1}{J_2} = \frac{\sigma_1 E_1}{\sigma_2 E_2} = \frac{\sigma_1 \varepsilon_2}{\sigma_2 \varepsilon_1} \tag{7}$$

In this special case where $\sigma_1\varepsilon_2 = \sigma_2\varepsilon_1$, the interface has zero density of free charges. However, if $\sigma_1\varepsilon_2 \neq \sigma_2\varepsilon_1$, the difference in current densities implies that the interface is actually charged. It will also be charged if $\sigma_1 = 0$ and $\sigma_2 > 0$.

Maxwell (20) derived an analytical solution for the conductivity σ of a dilute suspension of spherical particles:

$$\frac{\sigma - \sigma_2}{\sigma + 2\sigma_2} = \frac{p(\sigma_1 - \sigma_2)}{\sigma_1 + 2\sigma_2} \tag{8}$$

where p is the volume fraction of spheres, subscript 1 is for the particle and 2 for the medium. It was extended by Wagner (21) to ac cases and by Fricke (22, 23) to the case of oblate or prolate spheroids (Maxwell-Fricke equation):

$$\frac{\bar{\sigma} - \bar{\sigma}_2}{\bar{\sigma} + \gamma\bar{\sigma}_2} = \frac{p(\bar{\sigma}_1 - \bar{\sigma}_2)}{\bar{\sigma}_1 + \gamma\bar{\sigma}_2} \tag{9}$$

where γ is a shape factor equal to 2 for spheres and 1 for cylinders normal to the field.

Maxwell's equation is rigorous only for dilute concentrations, and Hanai (24) extended the theory for high volume fractions. The difference between the values predicted by the theories of Maxwell and Hanai is not pronounced, at least for the case of poorly conducting particles; e.g., for a volume concentration of $p = 0.5$, the suspension conductivities differ by only 11%. Experimental data agree with Maxwell (25). For more details, see Schwan and Takashima (26).

In order to better model biological systems such as blood or cell suspensions, this theory has been modified to apply to, e.g., dilute suspensions of membrane covered spheres, where membrane thickness d is much less than large sphere radius a. Fricke (27) gives the expression for the complex conductivity of one membrane covered sphere:

$$\bar{\sigma}_1 = \frac{\bar{\sigma}_i - (2d/a)(\bar{\sigma}_i - \bar{\sigma}_{sh})}{(1 + d/a)(\bar{\sigma}_i - \bar{\sigma}_{sh})/\bar{\sigma}_{sh}} \tag{10}$$

where subscript i is for the sphere material and sh is for the sheath membrane. This equation is inserted into the Maxwell-Fricke equation to yield the total expression for a dilute suspension of membrane-covered spheres.

Pauly and Schwan (5, 17, 28) adapted these equations to the case of a cell suspension with cell membranes dominated by a membrane capacitance C_m:

$$\Delta\varepsilon' = 9paC_m/4\varepsilon_0 \quad (11)$$

$$\sigma_s = \sigma_2(1 - 3p/2) \quad (12)$$

$$\tau = aC_m(1/2\sigma_2 + 1/\sigma_1) \quad (13)$$

where subscript 1 is for the particle and 2 for the medium. These Pauly-Schwan equations correspond to a large dispersion at radio frequencies due to cell membrane charging effects and a small dispersion at higher frequencies due to the different conductivities of the cytoplasm and the extracellular liquids. The equations also assume that the membrane conductance is zero, and they apply for small values of p. For equations including membrane conductance, see Schwan (5). Schwan and Morowitz (29) extended the theory to small vesicles of radii 100 nm. With even smaller particles, the two dispersion regions overlap in frequency (30).

Dipolar Relaxation Effects

Some molecules are polar, e.g., water and many proteins. Permanent dipoles will be randomly oriented, but if an external electric field is applied, they will reorient statistically. Induced dipoles will have the direction of the applied field. The rotational force exerted by the field on a permanent dipole is defined by the torque:

$$\tau = q\overline{L} \times \overline{E} \quad (14)$$

where q is the charge, L is charge separation, and E is the electric field strength.

The relation between the polarization and the molecular structure of a nonpolar medium is given by the Clausius-Mosotti equation:

$$\frac{\varepsilon_r - 1}{\varepsilon_r + 2} = \frac{N\alpha}{3\varepsilon_0} \quad (15)$$

where N is the volume density of atoms or molecules, and α is the polarizability. Debye (19) derived an equation where also the contribution from polar molecules is included:

$$\frac{\varepsilon_r - 1}{\varepsilon_r + 2} = \frac{N_A}{3v_m}\left(\alpha + \frac{p^2}{3kT}\right) \quad (16)$$

where v_m is the molar volume, p is the dipole moment, and N_A is Avogadro's constant. The kT factor is due to the statistical distribution of polar molecules causing the orientational polarization. Intermolecular interactions are neglected in Eq. 16, so it is in best agreement with very diluted systems such as gases. Kirkwood (31), Onsager (32), and others later extended the theory to more concentrated systems.

The orientation of polar molecules in an applied electric field requires time and, hence, causes a dispersion of the type given in Eq. 3, which is valid for any one time constant relaxation mechanism. However, a distribution of time constants will often be found due to molecular inhomogeneity and nonspherical shape. The time constant is proportional to the cube of the radius of the molecules, and typical characteristic frequencies are, e.g., 15–20 GHz for water and 400–500 MHz for simple amino acids (j). Proteins add another dispersion typically centered in the 1–10 MHz range. It is of smaller magnitude than the β-dispersion (26).

Counterion Relaxation Effects

Schwartz (11) used theories of electric double layers to describe the measured α-dispersion of particle suspensions. He considered the case where counterions are free to move laterally but not transversally on the particle surface. When an external field is applied, the system will be polarized since the counterions will be slightly displaced relative to the particle. The re-establishment of the original counterion atmosphere after the external field is switched off will be diffusion controlled, and the corresponding time constant according to Schwartz' theory is

$$\tau = \frac{a^2 e}{2\mu kT} \quad (17)$$

where a is the radius of the sphere, e is the elementary charge, and μ is counterion mobility. This will lead to a permittivity dispersion.

Improvement of the Schwartz' theory, e.g., to also account for diffusion of ions in the bulk solution near the surface, has been presented in a large number of articles (see e.g., the review by Mandel and Odijk (33)). A more detailed discussion of this work is given elsewhere in this encyclopedia.

Although Schwartz' theory has obvious limitations, it is simple to use and will in many cases provide an acceptable estimate of what to expect from dielectric measurements. As an example, we used Schwartz' theory to analyze data from four-electrode measurements on 6-μm-thick microporous polycarbonate membranes in electrolyte solution (34). The membranes had 3×10^8 cylindrical pores per cm^2 with a pore diameter of 100 nm. Takashima had earlier modified Schwartz' equations to apply to a suspension of long cylinders subject to an external field along their major axis (35):

$$\Delta\bar{\varepsilon} = \frac{e^2 q_s a^2}{bkT}\frac{9\pi p}{2(1+p)^2}\frac{1}{1+j\omega\tau} \quad \text{if } a \gg b \quad (18)$$

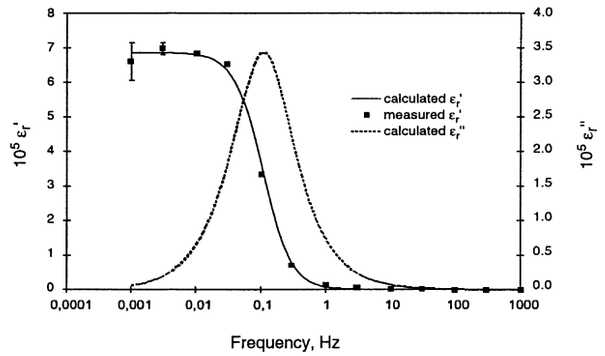

Fig. 4 Dielectric dispersion of a microporous polycarbonate membrane in electrolyte solution. (From Ref. 34.)

where q_s is the surface density of charged groups, a and b are cylinder length and radius, respectively, and p is the volume fraction of cylinders. The corresponding relaxation time τ is given by the counterion mobility μ:

$$\tau = \frac{(a^2 + b^2)e}{2\mu kT} \approx \frac{a^2 e}{2\mu kT} \tag{19}$$

The approximation in Eq. 19 is valid if $a >> b$. Fig. 4 shows the measured dispersion together with the calculated real and imaginary parts from Eq. 18. Any measured dielectric loss is not plotted in the figure, as it was totally hidden in the much greater background conductance of the KCl solution used in the experiment.

In the calculation of the counterion mobility μ, a minimum distance of 0.51 nm between counterion and surface charge and an effective relative permittivity of 22 were used in order to fit the calculated curves to the measured data. It is concluded in the article that these values seem sensible and are in agreement with Pethig (36), who reports that permittivity values are expected to drop rapidly at distances <0.6 nm.

CELLS AND TISSUE

Cell suspensions will typically exhibit a significant β-dispersion in the radio frequency range. This is due to the Maxwell-Wagner effect at the interface between the intra- or extracellular solution and the phospholipid membrane (26, 37). In addition, the water molecules will cause a γ-dispersion, and any proteins or other macromolecules will produce dispersions at frequencies ranging from the α- through the γ-range, depending on the size and charge of the molecules. Water bound to the protein will also cause a δ-dispersion. The β-dispersion exhibited by the proteins are of much smaller magnitude than that caused by the cell membranes, and the characteristic frequency is typically somewhat higher. The protein relaxation will hence typically appear as a small tail to the large cell membrane β-dispersion. Contribution to this tail may also come from the dispersion of organelles, which because of their smaller size, have a higher characteristic frequency than the main cell membrane.

Cell suspensions will also display a large α-dispersion because of counterion relaxation on the cell surface. However, whole blood does curiously not display any α-dispersion (38, 39), whereas cell ghosts do (40). Many cells also possess channels or tubular systems such as muscle cells. Fatt (41) argued that the measured α-dispersion of muscle cells originates from polarization of the entrance of these channel systems. This was discussed by Foster and Schwan (28), who concluded that probably both the polarization of the channel system and counterion polarization at the cell surface were responsible for the α-dispersion.

Tissue is a highly inhomogenuous material, and it is obvious that interfacial processes play an important role in the electrical properties of tissue. It is also generally an

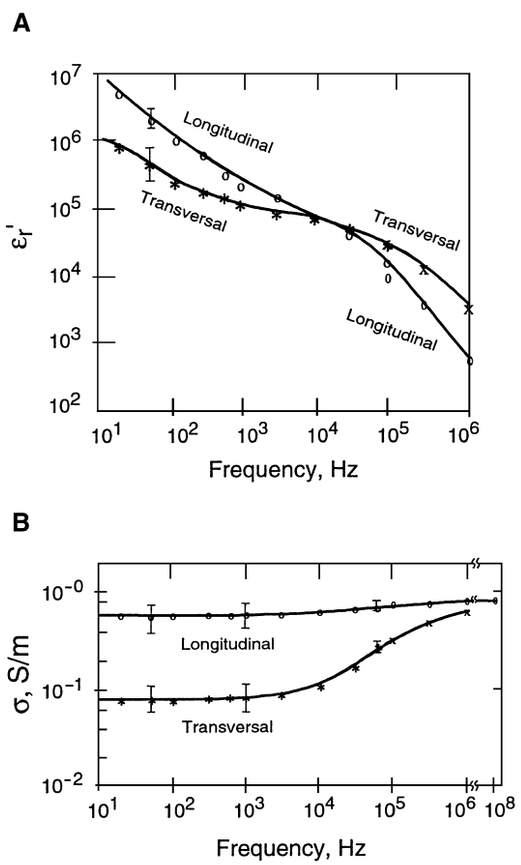

Fig. 5 Anisotropy of relative permittivity and conductivity of dog skeletal muscle. (Redrawn from Ref. 42.)

anisotropic medium because of the orientation of cells, macromembranes, and organs.

Epstein and Foster (42) measured on dog excised skeletal muscle. From the results in Fig. 5, the low-frequency conductance ratio between transversal and longitudinal directions is about 1:8. The conductance is also less frequency dependent in the longitudinal direction, indicating that it is probably dominated by direct current paths with few membranes. As mentioned above, the α-dispersion of muscle tissue is probably due to a combination of counterion relaxation and polarization of the sarcotubular membrane system. Gap junctions can also produce an α-dispersion in some tissues, e.g., in porcine liver at about 7 Hz, which vanishes completely when the gap junctions close (43). The very apparent β-dispersion in the transversal measurements is most likely of the interfacial Maxwell-Wagner type. A number of studies have also been carried out on postmortem changes in muscle and other tissues, with possible applications ranging from meat quality assessment to organ state evaluation in transplantations (44–48). Relating electrical measurements to knowledge about the physiological processes occurring after excision is very useful and has added to the understanding of the mechanisms behind the dielectric dispersions.

Human skin is another example where bioimpedance measurements have proved to be of direct practical value. Knowledge about the dielectric properties of skin is essential when producing skin electrodes, whether it is for ECG or, e.g., defibrillation. A number of studies have also been dedicated to the possible use of skin impedance measurements for diagnostic purposes such as skin hydration measurements or the detection of skin reactions or diseases (49–55).

The permittivity and resistivity of skin is shown in Fig. 6 (56). The uppermost, dead layer of the skin, the stratum corneum, is separated from the viable part of the skin in this figure, because the stratum corneum has electrical properties that differ greatly from that of viable skin. The stratum corneum is only about 15 μm thick on most skin sites, but nevertheless totally dominates the measured skin impedance at low frequencies with its resistivity, which is about four orders of magnitude higher than that of the viable skin layers. Hence, for typical skin impedance measurements, the stratum corneum will dominate in the measurements up to a few kilohertz, and at higher frequencies, the influence from viable skin will be significant (57). The dc conductance of skin is partly due to the electrolyte solution (sweat) in the sweat ducts and partly to free ions in the skin (58, 59). The stratum corneum displays a very broad α-dispersion, which is probably due to macromolecules and counterions on very diverse cell sizes and shapes (see Fig. 6). It also shows a pronounced β-dispersion, which would be expected since the stratum corneum consists mainly of compressed, keratinized cell membranes. Viable skin has electrical properties those resembles that of other living tissues and hence usually displays more separated α- and β-dispersions (54). The interface between the stratum corneum and the viable skin will also give rise to a Maxwell-Wagner type of dispersion in the β-range.

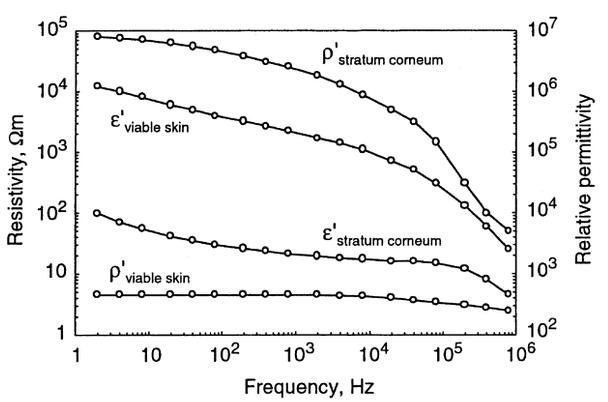

Fig. 6 Average resitivities and relative permittivities in the stratum corneum and viable skin. (Redrawn from Ref. 56.)

DATA AND MODELS

The choice of how to present bioimpedance data is most crucial. Presented as material constants, such as complex permittivity in a Cole-Cole plot, the impression and even interpretation may be entirely different from when the data are presented, let's say, as conductance and susceptance in a Bode plot. The way of presentation should hence always be chosen with great care, and data should preferably be presented more than one way before any conclusions are drawn.

The most fundamental way of presenting impedance data from measurements at one single frequency is according to

$$\overline{Z} = R - jX \text{ or } \overline{Y} = G + jB \tag{20}$$

or alternatively as, e.g., complex permittivity or conductivity if the geometry is known. Even at this simple level, the choice is decisive, since the impedance values are linked to the situation where conduction of free ions and electrical polarization physically occurs in series, while the admittance values are linked to a parallel model. Hence resistance R is not the inverse of conductance G, and reactance X is not the inverse of susceptance B, and by choosing either of the two expressions in Eq. 20, a physical model of the processes involved is inevitably selected at the same time.

It is customary in the physical sciences to regard dielectrica as materials placed between the plates of a capacitor and thus subject to an electric field. This implies that conductance and capacitance physically are in parallel, and it is natural to present the electrical properties in terms of conductivity σ' and permittivity ε'. As a matter of fact, there are no corresponding terms in use for the volume-specific quantities of R and X. The term ''resistivity'' is commonly defined as the quantity $1/\sigma'$, which is different from the quantity R per volume unit. Moreover, many fluids have frequency-independent properties σ' and ε' over a very broad frequency range, e.g., electrolytes. Thus, their quantities R and X per volume unit change with frequency in a manner that hides the simple underlying mechanism responsible for the frequency independence of ε' and σ' and display a relaxation frequency that changes with salt concentration and has no physical significance.

In the presence of one relaxation process, the electrical properties can be represented by either a parallel G-C network in series with a resistor or a capacitor or a series R-C network parallel to a C or G, depending on whether one prefers to get a semicircle either in the admittance and impedance plane or in the dielectric plane. Thus suspensions of spherical cells of fairly uniform size are well presented by a single relaxation time (5), and a semicircle in the admittance plane is proper since the parallel component is the medium's electrolyte and its capacitance can be neglected over most of the frequency range (except at very high frequencies). When the cells deviate from the spherical shape, the agreement is slightly broadened since a spectrum of time constants becomes apparent.

Significant deviation from one time constant may require a second relaxation process. See e.g., Fricke et al. (60), where the particle axial ratio 1:4 suggests two time constants that differ by the same ratio. Better agreement with biological systems has often been found by incorporating elements with a frequency-independent phase angle, so-called *constant phase elements* (CPE). These CPEs can be interpreted as being due to a distribution of relaxation time constants, e.g., because of differences in cell size and shape, and it has been shown that almost any logarithmically symmetrical distribution of time constants will produce an apparent constant phase angle element (28). Hence the high-frequency data on liver presented by Stoy et al. (16) can be modeled by a constant phase element or in a more explanatory way by two relaxation terms representing total cell and mitochondrial compartments.

A constant phase admittance can be obtained by giving the conductance and susceptance the following frequency dependence:

$$G_{cpe} = G_{\omega=1}\omega^m \quad \text{and} \quad B_{cpe} = B_{\omega=1}\omega^m \tag{21}$$

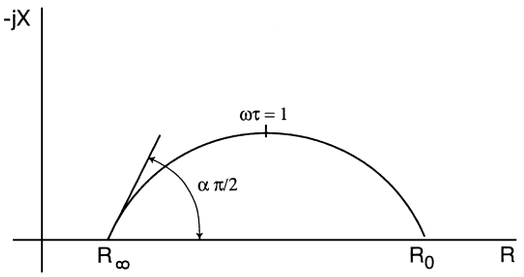

Fig. 7 Cole plot in the impedance plane.

According to Fricke's law (61) there is a correlation between the frequency exponent m and the phase angle φ in many electrolytic systems. Schwan (18) published electrode data in the frequency range 20 Hz to 200 kHz and noticed m to vary with frequency. Howevere, it can be shown that Fricke's law is not in agreement with the Kramers-Kronig transforms if m is frequency dependent (62).

An empirical equation for impedance was proposed by Cole in 1940 (63) and for complex permittivity by Cole and Cole in 1941 (64). The impedance version is shown in Eq. 22, and the corresponding Cole plot in the impedance plane is shown in Fig. 7.

$$\overline{Z} = R_\infty + \frac{R_0 - R_\infty}{1 + (j\omega\tau)^\alpha} \tag{22}$$

The subscripts for R refer to frequency, τ is a time constant, e.g., the mean relaxation time in a distribution of time constants, and $\alpha(\pi/2)$ is the constant phase angle. The constant $1 - \alpha$ may also be viewed as describing the width of the distribution of time constants. Because of their simplicity, the Cole- and Cole-Cole models have been used extensively in the literature. It should be noted that a circular arc locus is not proof of any accordance with Fricke's law or the Cole equation. Data should be checked for Fricke compatibility. This, and the use of models and data presentation in general is broadly covered in Grimnes and Martinsen (4).

DISPERSION AND ELECTROROTATION

Particles suspended in a liquid may experience a torque in a rotating E-field. A dipole is induced in the particle, and since this polarization process is not immediate, the induced dipole will lag the external field and a frequency-dependent torque will exist. This torque is dependent on a relaxation time constant identical to the time constant in the theory for β-dispersion (65), and is given by (subscript 1 is for the particle and 2 for the medium):

$$\Gamma = -4\pi a^3 \varepsilon_2 \nabla E^2 U'' \tag{23}$$

where U'' is the imaginary part of the Clausius-Mossotti factor:

$$\overline{U} = \frac{\bar{\varepsilon}_1 - \bar{\varepsilon}_2}{\bar{\varepsilon}_1 + 2\bar{\varepsilon}_2} = \frac{\bar{\sigma}_1 - \bar{\sigma}_2}{\bar{\sigma}_1 + 2\bar{\sigma}_2} \tag{24}$$

Hence, a torque will exist if $U'' \neq 0$.

Electrorotation of biological cells at radio frequencies produce results that are consistent with those obtained with dielectric spectroscopy. However, Arnold et al. (66) reported on a low frequency peak in the rotation spectrum of latex particles in addition to the expected Maxwell-Wagner related peak in the upper kilohertz range (Fig. 8).

Under the assumptions that this is due to dispersive behavior of the particle itself and that the frequency is so low that only the real part of the medium conductivity has to be considered, they find that U'' is given by

$$U'' = \frac{3\sigma_2 \Delta\sigma_1 \omega\tau}{(\sigma_{1t} + 2\sigma_2)^2 + (\omega\tau)^2(\sigma_1 + \sigma_{1t} + \sigma\tau_2)^2} \tag{25}$$

where the term σ_{1t} describes the low-frequency limit of the particle conductivity, and $\Delta\sigma_1$ is the increment (usually positive) in conductivity due to the dispersion.

However Eq. 25 predicts a counterfield rotation in case of the usual type of dispersion where the conductivity increases with frequency ($\Delta\sigma_1 > 0$), whereas the measurements gave a cofield rotation peak. Arnold et al. (66) suggest two alternative explanations for this behavior. Firstly they point out that the inertia present in the dielectric because of the effective mass of the moving particle, could give such a negative dispersion. They do not sustain this theory, however, since it would predict dispersion at a frequency about three orders of magnitude higher than the experimental results indicate. Instead they present a possible explanation, which will not be predicted by Eq. 25 since the permittivity ε_2 of the medium was assumed to be frequency independent. The ionic double layer of counterions attracted to charges groups on the particle surface will change the effective permittivity of the medium next to the particle. When the particle rotates, only the closest adsorbed ions, i.e., the part of the diffuse double layer situated inside the shear plane, will move with the particle. This gives a qualitative understanding that dielectric spectroscopy will give results reflecting particle properties as seen from the outside of the double layer, whereas particle rotation measurements will reflect the properties of the particle with closely adsorbed ions only. Hence, the counterion relaxation effects and the spatial changes in permittivity in the diffuse double layer must be taken into account when calculating particle rotation.

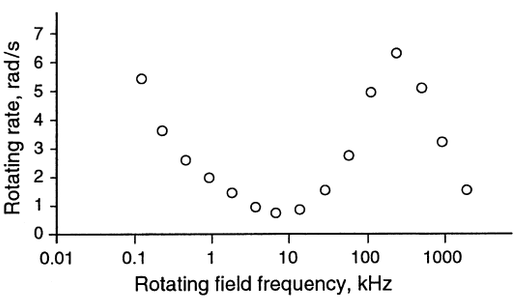

Fig. 8 Rotation spectrum of 5.29-μm latex particles in 7 μS/cm medium. (Redrawn from Ref. 66.)

Zhou et al. (67) reported the same anomalous low frequency rotation peak in their measurements on polystyrene beads. They give the following differential equation describing the displacement of counterions in the inner double layer caused by an applied field $Ee^{j\omega t}$:

$$\frac{d(\delta_q)}{dt} + \left(\frac{K_s}{r} + \sigma_2\right)\frac{\delta_q}{\varepsilon_2} = \frac{K_s}{r}E \tag{26}$$

where K_s is the surface conductivity of the equilibrium double layer. The resulting induced dipole moment has magnitude of the order $r^3\delta_q$, where r is particle radius and δ_q is the change in charge per unit area of the double layer caused by the external field. This induced moment goes through a dispersion and decreases with increasing frequency about a characteristic frequency f_{c1} given by

$$f_{c1} = \frac{1}{2\pi}\left(1 + \frac{K_s}{\sigma_2 r}\right)\Big/\frac{\varepsilon_2}{\sigma_2} \tag{27}$$

Since the induced dipole moment decreases with frequency, it will result in a counterfield electrorotaion peak centered around f_{c1}. For the system of 6-μm polystyrene beads in a 1 mS/m medium used by Zhou et al. (67), f_{c1} is found to be of the order 450 kHz.

Zhou et al. (67) further point out that the initial rapid displacement of counterions near to the surface of the particle is counteracted by changes in both counterion and co-ion densities beyond the electrical double layer. The steady state condition is thus approached with a characteristic time-constant equal to that required for an ion to diffuse through a distance of the order of the particle radius. This process will give a characteristic frequency:

$$f_{c2} = \frac{1}{2\pi}\frac{D}{r^2} \tag{28}$$

where D is the ion diffusivity. The effective induced dipole moment will increase with increasing frequency, leading to co-field electrorotation. In their system f_{c2} will be about 35 Hz.

Grosse and Shilov (68) propose electro-osmosis as an alternative explanation of the co-field rotation. They show that the main cause of the particle rotation at low fre-

quencies is the electroosmotic velocity of the electrolyte inside the double layer, rather than the torque exerted by the rotating electric field on the imaginary part of the induced dipole moment. Separate expressions for the two mechanisms involved, dipole-electric field interaction and electroosmosis, are given in the paper. The analytical solution presented by Grosse and Shilov (68) is too comprehensive to be presented here, and we hence refer the reader to the original article. Recently, Georgieva et al. (69) and others have presented experimental results that are consistent with the theory of Grosse and Shilov.

REFERENCES

1. Höber, R. Eine zweites verfahren die leitfähigkeit im inner von zellen zu messen. Pfluegers Arch. Gesamte Physiol. Menschen Tiere **1912**, *148*, 189.
2. Höber, R. Eine Metode, die electrische leitfähigkeit im inner von zellen zu messen. Pfluegers Arch. Gesamte Physiol. Menschen Tiere **1910**, *133*, 237.
3. Fricke, H. The electric capacity of suspensions with special reference to blood. J. Gen. Physiol. **1925**, *9*, 137–152.
4. Grimnes, S.; Martinsen, ∅.G. *Bioimpedance and Bioelectricity Basics*; Academic Press: San Diego, 2000.
5. Schwan, H.P. Electrical Properties of Tissue and Cell Suspensions. In *Advances in Biological and Medical Physics*; Lawrence, J.H., Tobias, C.A., Eds.; Acad. Press: New York, 1957; Vol. V, 147–209.
6. Cole, K.S. *Membranes, Ions and Impulses*; University of California Press: Berkeley, 1972.
7. Schwan, H.P. Electrical properties of muscle tissue at low frequencies. ZS. F. Naturforsch. **1954**, *9B*, 245.
8. Falk, G.; Fatt, P. Linear electrical properties of striated muscle fibers observed with intracellular electrodes. Proc. R. Soc. London, Ser. B **1964**, *160*, 69–123.
9. Schwan, H.P.; Schwarz, G.; Maczuk, J.; Pauly, H. On the low-frequency dielectric dispersion of colloidal particles in electrolyte solution. Phys. Chem. **1962**, *66*, 2626.
10. Schwan, H.P.; Maczuk, J. In *Electrical Relaxation Phenomena of Biological Cells and Colloidal Particles at Low Frequencies*. Proc. of the First National Biophysics Conf.; Yale University Press, 1959; 348–355.
11. Schwartz, G. A theory of the low frequency dispersion of colloid particles in electrolyte solution. J. Phys. Chem. **1962**, *66*, 2636–2642.
12. Rajewsky, B.; Schwan, H.P. The dielectric constant and conductivity of blood at ultrahigh frequencies. Naturwissenschaften **1948**, *35*, 315.
13. Schwan, H.P. Mechanism responsible for electrical properties of tissues and cell suspensions. Med. Prog. Technol. **1993**, *19*, 163–165.
14. Fishman, H.M.; Poussart, D.; Moore, L.E.; Siebenga, E. K+ conduction description from the low frequency impedance and admittance of squid axon. J. Membr. Biol. **1977**, *32*, 255–290.
15. Fishman, H.M. Linearity, Admittance and Ion Conduction in Nerve Membrane. In *Interactions Between Electromagnetic Fields and Cells*; Chiabrera, A., Nicolini, C., Schwan, H.P., Eds.; Plenum Press: New York, 1985; Vol. 97, 339–355.
16. Stoy, R.D.; Foster, K.R.; Schwan, H.P. Dielectric properties of mammalian tissues from 0.1 to 100 MHz: a summary of recent data. Phys. Med. Biol. **1982**, *27*, 501–513.
17. Pauly, H.; Schwan, H.P. Über die Impedanz einer Suspension von Kugelformigen Teilchen mit einer Schale. Z. Naturforsch., B **1959**, *14B*, 125–131.
18. Schwan, H.P. Determination of Biological Impedances. In *Physical Techniques in Biological Research*; Nastuk, W.L., Ed.; Academic Press: New York, 1963; Vol. 6, 323–406.
19. Debye, P. *Polar Molecules*; Dover: New York, 1929; 45.
20. Maxwell, J.C. *Treatise on Electricity and Magnetism*; Oxford University Press, 1873.
21. Wagner, K.W. Explanation of the dielectric fatigue phenomena on the basis of Maxwell's concept. Arch. Elecktro. Technol. **1914**, *2*, 371.
22. Fricke, H. A mathematical treatment of the electrical conductivity and capacity of disperse systems. I. The electrical conductivity of a suspension of homogeneous spheroids. Phys. Rev. **1924**, *24*, 575–587.
23. Fricke, H. A mathematical treatment of the electrical conductivity and capacity of disperse systems. II. The capacity of a suspension of conducting spheroids surrounded by a non-conducting membrane for a current of low frequency. Phys. Rev. **1925**, *26*, 678–681.
24. Hanai, T. Theory of the dielectric dispersion due to the interfacial polarization and its application to emulsion. Kolloid-Z. **1960**, *171*, 23–31.
25. Cole, K.S.; Li, C.L.; Bak, A.F. Electrical analogues for tissues. Exp. Neurol. **1969**, *24*, 459–473.
26. Schwan, H.P.; Takashima, S. Electrical conduction and dielectric behavior in biological systems. Encycl. Appl. Phys. **1993**, *5*, 177–200.
27. Fricke, H. The complex conductivity of a suspension of stratified particles of spherical cylindrical form. J. Phys. Chem. **1955**, *59*, 168.
28. Foster, K.R.; Schwan, H.P. Dielectric properties of tissue. CRC Crit. Rev. Biomed. Eng. **1989**, *17*, 25–104.
29. Schwan, H.P.; Morowitz, H.J. Electrical properties of the membranes of the pleuro-pneumonia-like organism A5969. Biophys. J. **1962**, *2*, 295.
30. Schwan, H.P.; Takshima, S.; Miyamoto, V.K.; Stoeckenius, W. Electrical properties of phospholipid vesicles. Biophys. J. **1970**, *10*, 1102.
31. Kirkwood, J.G. The dielectric polarization of polar liquids. J. Chem. Phys. **1939**, *7*, 911.
32. Onsager, L.J. Electric moments of molecules in liquids. Am. Chem. Soc. **1936**, *58*, 1486–1493.
33. Mandel, M.; Odijk, T. Dielectric properties of polyelectrolyte solutions. Ann. Rev. Phys. Chem. **1984**, *35*, 75–108.
34. Martinsen, ∅.G.; Grimnes, S.; Karlsen, J. Low frequency dielectric dispersion of microporous membranes in electrolyte solution. J. Colloid Interface Sci. **1998**, *199*, 107–110.

35. Takashima, S. *Electrical Properties of Biopolymers and Membranes*; Adam Hilger: Bristol, 1989.
36. Pethig, R. *Dielectric and Electronic Properties of Biological Materials*; Wiley: New York, 1979.
37. Pethig, R.; Kell, D.B. The passive electrical properties of biological systems: their significance in physiology, biophysics and biotechnology. Phys. Med. Biol. **1987**, *32*, 933–970.
38. Schwan, H.P.; Bothwell, T.P.; Wiercinski, F.J. Electrical properties of beef erythrocyte suspensions at low frequencies. Fed. Proc. Am. Soc. Exp. Biol. **1954**, *13*, 15.
39. Schwan, H.P.; Bothwell, T.P. Electrical properties of the plasma membrane of erythrocytes at low frequencies. Nature **1956**, *178*, 265.
40. Schwan, H.P.; Carstensen, E.L. Dielectric properties of the membrane of lysed erythrocytes. Science **1957**, *125*, 985.
41. Fatt, P. An analysis of the transverse electrical impedance of striated muscle. Proc. R. Soc. London, Ser. B **1964**, *159*, 606–651.
42. Epstein, B.R.; Foster, K.R. Anisotropy in the dielectric properties of skeletal muscles. Med. Biol. Eng. Comput. **1983**, *21*, 51.
43. Gersing, E. Impedance spectroscopy on living tissue for determination of the state of organs. Bioelectrochem. Bioenerg. **1998**, *45* (2), 145–149.
44. Bozler, E.; Cole, K.S. Electric impedance and phase angle of muscle in rigor. J. Cell. Comp. Physiol. **1935**, *6*, 229–241.
45. Gheorghiu, M.; Gersing, E.; Gheorghiu, E. Quantitative analysis of impedance spectra of organs during ischemia. Ann. N.Y. Acad. Sci. **1999**, *873*, 65–71.
46. Ollmar, S. Noninvasive monitoring of transplanted kidneys by impedance spectroscopy – a pilot study. Med. Biol. Eng. Comput. **1997**, *35*, 336, (suppl.).
47. Schäfer, M.; Schlegel, C.; Kirlum, H.-J.; Gersing, E.; Gebhard, M.M. Monitoring of damage to skeletal muscle tissue caused by ischemia. Bioelectrochem. Bioenerg. **1998**, *45*, 151–155.
48. Martinsen, ∅.G.; Grimnes, S.; Mirtaheri, P. Non-invasive measurements of post mortem changes in dielectric properties of haddock muscle – a pilot study. J. Food Eng. **2000**, *43* (3), 189–192.
49. Martinsen, ∅.G.; Grimnes, S.; Karlsen, J. Electrical methods for skin moisture assessment. Skin Pharmacol. **1995**, *8* (5), 237–245.
50. Martinsen, ∅.G.; Grimnes, S.; Henriksen, I.; Karlsen, J. Measurement of the effect of topical liposome preparations by low frequency electrical susceptance. Innov. Technol. Biol. Med. **1996**, *17* (3), 217–222.
51. Martinsen, ∅.G.; Grimnes, S. On using single frequency electrical measurements for skin hydration assessment. Innov. Technol. Biol. Med. **1998**, *19* (5), 395–399.
52. Emtestam, L.; Nicander, I.; Stenstrøm, M.; Ollmar, S. Electrical impedance of nodular basal cell carcinoma: a pilot study. Dermatology **1998**, *197*, 313–316.
53. Lahtinen, T.; Nuutinen, J.; Alanen, E.; Turunen, M.; Nuortio, L.; Usenius, T.; Hopewell, J.W. Quantitative assessment of protein content in irradiated human skin. Int. J. Radiat. Oncol., Biol., Phys. **1999**, *43*, 635–638.
54. Ollmar, S. Methods for information extraction from impedance spectra of biological tissue, in particular skin and oral mucosa – a critical review and suggestions for the future. Bioelectrochem. Bioenerg. **1998**, *45*, 157–160.
55. Nicander, I.; Ollmar, S.; Eek, A.; Lundh Rozell, B.; Emtestam, L. Correlation of impedance response patterns to histological findings in irritant skin reactions induced by various surfactants. Br. J. Dermatol. **1996**, *134*, 221–228.
56. Yamamoto, T.; Yamamoto, Y. Electrical properties of the epidermal Stratum corneum. Med. Biol. Eng. Comput. **1976**, *14*, 592–594.
57. Martinsen, ∅.G.; Grimnes, S.; Haug, E. Measuring depth depends on frequency in electrical skin impedance measurements. Skin Res. Technol. **1999**, *5*, 179–181.
58. Grimnes, S. Pathways of ionic flow through human skin in vivo. Acta Derm.-Venereol. (Stockh) **1984**, *64*, 93–98.
59. Martinsen, ∅.G.; Grimnes, S.; Sveen, O. Dielectric properties of some keratinised tissues. Part 1: stratum corneum and nail in situ. Med. Biol. Eng. Comput. **1997**, *35*, 172–176.
60. Fricke, H.; Schwan, H.P.; Li, K.; Bryson, V. A dielectric study of the low-conductance surface membrane in E Coli. Nature **1956**, *177*, 134.
61. Fricke, H. Theory of electrolytic polarization. Philos. Mag. **1932**, *14*, 310–318.
62. Daniel, V.V. *Dielectric Relaxation*; Academic Press: New York, 1967.
63. Cole, K.S. Permeability and impermeability of cell membranes for ions. Cold Spring Harbor Symp. Quant. Biol. **1940**, *8*, 110–122.
64. Cole, K.S.; Cole, R.H. Dispersion and adsorption in dielectrics. I. Alternating current characteristics. J. Chem. Phys. **1941**, *9*, 341–351.
65. Schwan, H.P. Dielectric properties of the cell surface and biological systems. Stud. Biophys. **1985**, *110*, 13–18.
66. Arnold, W.M.; Schwan, H.P.; Zimmermann, U. Surface conductance and other properties of latex particles measured by electrorotation. J. Phys. Chem. **1987**, *91*, 5093–5098.
67. Zhou, X.-F.; Markx, G.H.; Pethig, R.; Eastwood, I.M. Differentiation of viable and non-viable bacterial biofilms using electrorotation. Biochim. Biophys. Acta **1995**, *1245*, 85–93.
68. Grosse, C.; Shilov, V.N. Theory of the low-frequency electrorotation of polystyrene particles in electrolyte solution. J. Phys. Chem. **1996**, *100*, 1771–1778.
69. Georgieva, R.; Neu, B.; Shilov, V.N.; Knippel, E.; Budde, A.; Latza, R.; Donath, E.; Kiesewetter, H.; Bäumler, H. Low frequency electrorotation of fixed red blood cells. Biophys. J. **1998**, *74*, 2114–2120.